Methane Reforming

Deutsche Ausgabe: DOI: 10.1002/ange.201602489
Internationale Ausgabe: DOI: 10.1002/anie.201602489

Dry Reforming of Methane on a Highly-Active Ni-CeO_2 Catalyst: Effects of Metal-Support Interactions on C–H Bond Breaking

Zongyuan Liu, David C. Grinter, Pablo G. Lustemberg, Thuy-Duong Nguyen-Phan, Yinghui Zhou, Si Luo, Iradwikanari Waluyo, Ethan J. Crumlin, Dario J. Stacchiola, Jing Zhou, Javier Carrasco, H. Fabio Busnengo, M. Verónica Ganduglia-Pirovano, Sanjaya D. Senanayake,* and José A. Rodriguez**

Abstract: *Ni-CeO_2 is a highly efficient, stable and non-expensive catalyst for methane dry reforming at relative low temperatures (700 K). The active phase of the catalyst consists of small nanoparticles of nickel dispersed on partially reduced ceria. Experiments of ambient pressure XPS indicate that methane dissociates on Ni/CeO_2 at temperatures as low as 300 K, generating CH_x and CO_x species on the surface of the catalyst. Strong metal–support interactions activate Ni for the dissociation of methane. The results of density-functional calculations show a drop in the effective barrier for methane activation from 0.9 eV on Ni(111) to only 0.15 eV on Ni/CeO_{2-x}(111). At 700 K, under methane dry reforming conditions, no signals for adsorbed CH_x or C species are detected in the C 1s XPS region. The reforming of methane proceeds in a clean and efficient way.*

Methane and CO_2 are both common components of natural and land-fill gas with great technological incentives to utilize both as reactants for the catalytic dry reforming process (DRM: $CH_4 + CO_2 \rightarrow 2\,CO + 2\,H_2$).[1,2] A review of the scientific literature indicates that there are four key issues that must be addressed to optimize the DRM process for industrial applications: 1) Improve CH_4 activation; 2) Improve CO_2 activation; 3) Obtain a better understanding of the reaction mechanism for the formation of CO and H_2; and 4) Avoid deactivation by carbon deposition.[1–3] The DRM process likely involves the following series of sequential reactions:

$CH_4(g) \rightarrow CH_{4-x}(a) + H(a)$ with $x = 1$–4

$CO_2(g) \rightarrow CO(a) + O(a)$

$C(a) + O(a) \rightarrow CO(g)$

$H(a) + H(a) \rightarrow H_2(g)$

The selective and stable conversion of CH_4 and CO_2 is challenging owing to their high gas-phase stability. Generally, it is accepted that the DRM process is limited primarily by the activation of C–H bonds.[1,4,5] Noble metals (Pt, Ru, Rh, Pd), although highly active for this reaction, at high temperatures suffer from rapid deactivation through particle sintering and chemical poisoning (C or O deposition).[1–4] Owing to its low cost, Ni dispersed on oxides is an attractive option as a catalyst for the DRM process.[1,6,7] Its use can be problematic owing to the high temperature of operation or deactivation by carbon deposition/encapsulation.[7–9] Herein, we report the behavior of a highly efficient, stable, and inexpensive Ni-CeO_2 catalyst for methane dry reforming at relatively low temperature (700 K). Strong metal–support interactions activate Ni for the dissociation of methane at a temperature as low as 300 K.

We prepared a NiO-CeO_2 mixed metal oxide catalyst and tested it for the DRM process. Figure 1 a displays an image of transmission electron microscopy (TEM) for the as-prepared catalyst. The catalyst contains very small particles of NiO dispersed on a solid solution of $Ce_{1-x}Ni_xO_{2-y}$. The overall composition of the system was 20 %-NiO/80 %-CeO_2. The NiO-CeO_2 precursor was activated by exposing it to a stream of 20 %H_2/He at 723 K. In situ measurements with time-resolved X-ray diffraction (Figure S1 in the Supporting Information) showed a transformation of NiO into Ni^0 and a minor expansion of the ceria lattice as a result of partial reduction. Figure 1 b shows data for the DRM process on this

[*] B. Sc. Z. Liu, B. Sc. S. Luo, Prof. J. A. Rodriguez
Department of Chemistry
State University of New York at Stony Brook,
Stony Brook, NY 11794 (USA)
E-mail: rodrigez@bnl.gov
Dr. D. C. Grinter, Dr. T.-D. Nguyen-Phan, Dr. I. Waluyo,
Dr. D. J. Stacchiola, Dr. S. D. Senanayake, Prof. J. A. Rodriguez
Chemistry Department
Brookhaven National Laboratory
Upton, NY 11973 (USA)
E-mail: ssenanay@bnl.gov
Dr. P. G. Lustemberg, Prof. H. F. Busnengo
Instituto de Fisica Rosario (IFIR), CONICET—Universidad Nacional de Rosario (Argentina)
Dr. Y. Zhou, Prof. J. Zhou
Department of Chemistry, University of Wyoming
Laramie, WY 82071 (USA)
Dr. E. J. Crumlin
Advanced Light Source, Lawrence Berkeley National Laboratory
Berkeley, CA 94720 (USA)
Dr. J. Carrasco
CIC Energigune
Albert Einstein 48, 01510 Miñano, Álava (Spain)
Dr. M. V. Ganduglia-Pirovano
Instituto de Catálisis y Petroleoquímica
CSIC
C/Marie Curie 2, 28049 Madrid (Spain)
E-mail: vgp@icp.csic.es

Supporting information for this article can be found under: http://dx.doi.org/10.1002/anie.201602489.

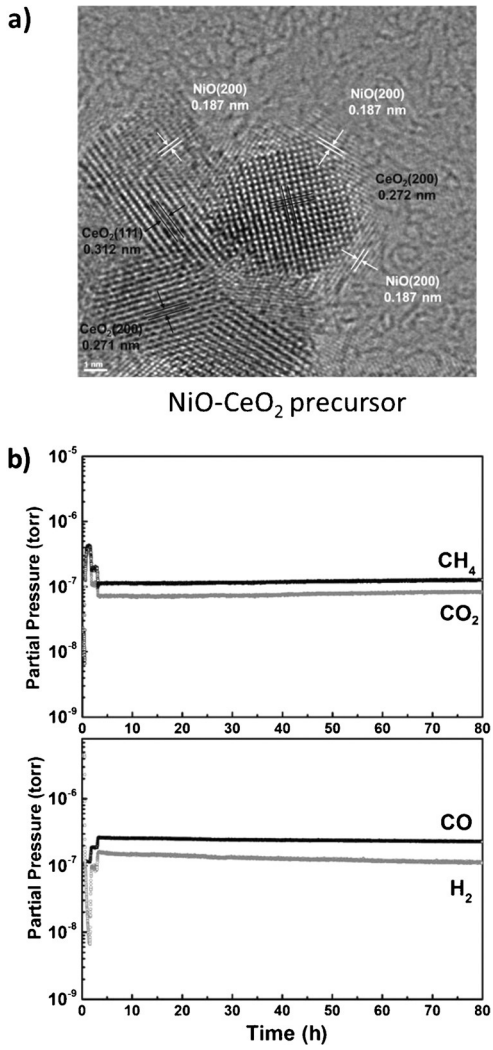

Figure 1. a) High-resolution TEM image of the NiO-CeO_2 precursor, b) Gas species derived from mass spectrum as a function of time for a Ni-CeO_{2-x} catalysts under methane dry reforming conditions for ca. 80 h. $T = 723$ K, a 10 cc m^{-} flow rate of a gas mixture containing 20% CO_2, 20% CH_4, and 60% He was used in this experiment.

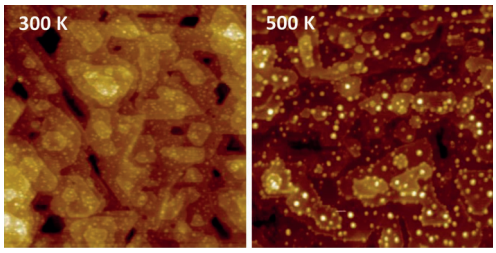

Figure 2. STM images for 0.1 ML Ni on CeO_2(111) after deposition at 300 K and annealing to 500 K. The area covered by each image is 120 nm × 120 nm.

annealing to 500 K. At 300 K, there is a large dispersion of Ni on ceria with small particles that have an average height of 0.23 nm and an average diameter of 1.80 nm. XPS indicated that most of the nickel was in a 2+ oxidation state.[10,11] Annealing to 500 K induced some sintering of the Ni particles and large fraction of the Ni migrated into the ceria substrate to form a $Ce_{1-x}Ni_xO_{2-y}$ solid solution.[12,13]

Figure 3 shows a series of XPS spectra collected for a Ni/CeO_2(111) surface under 100 mTorr of methane. In the C 1s

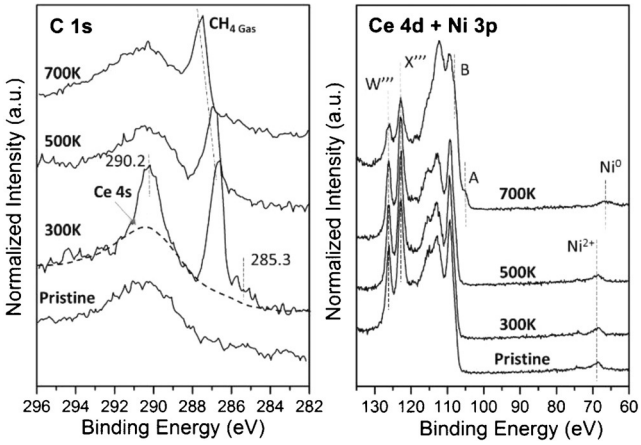

Figure 3. C 1s and Ce 4d + Ni 3p spectra of the Ni/CeO_2(111) ($\Theta_{Ni} \approx 0.1$ ML) surface under 100 mTorr of CH_4 at 300, 500, and 700 K.

Ni-ceria system. After exposure of the catalyst to the reactants, a steady-state is reached and the production of CO_2 and H_2 remains essentially constant after 80 h of operation. The total conversion was approximately 12%, a value close to the expected thermodynamic limit at a temperature of 723 K.[1a] The results of in situ X-ray diffraction indicated that the active phase of the catalyst contained small nanoparticles of Ni dispersed on partially reduced ceria. TEM images for the used catalyst showed a negligible amount of carbon on the surface.

To understand better the chemistry of the DRM process on a nickel-ceria catalyst, we used ambient-pressure X-ray photoelectron spectroscopy (XPS) to study the interaction of CH_4, CO_2 and a CH_4/CO_2 mixture with model Ni/CeO_2(111) surfaces. Figure 2 shows images of scanning tunneling microscopy (STM) collected after depositing 0.1 monolayers (ML) of nickel on a CeO_2(111) film at 300 K with subsequent region, at 300 K, there is a sharp peak for gaseous methane near 287 eV, a strong peak near 290.2 eV that can be attributed to adsorbed CO_x species,[14] and weak features at 285–286 eV that probably come from CH_x on the surface. This result implies that methane dissociates on the Ni/CeO_2 surface at room temperature. Some of the CH_4 molecules fully dissociate producing C atoms that eventually react with oxygen atoms of the ceria to yield CO_x species. In the corresponding spectrum for the Ce 4d and Ni 3p regions no sign is evident for a change in the oxidation state of Ce^{4+} and Ni^{2+} cations. At 700 K, no features for CO_x or CH_x are seen in the in the C 1s region, but a clear change is seen in the line shape of the Ce 4d region (formation of Ce^{3+}) and on the position of the Ni 3p peaks ($Ni^{2+} \rightarrow Ni^0$ transformation). We also detected the evolution of CO into gas phase during the exposure to CH_4 at this elevated temperature (Figure S2). Thus, there is a very fast reduction of the surface by methane.

Once the first hydrogen is removed from the reactant molecule, a quick $CH_3 \rightarrow CH_2 \rightarrow CH \rightarrow C$ transformation occurs on the surface and the deposited carbon reacts with oxygen atoms of the sample to yield gaseous CO. The H atoms abstracted from the reactant desorb as H_2 or H_2O.

We did similar experiments for a plain $CeO_2(111)$ surface observing some reduction of the system but the amount of Ce^{3+} formed at temperatures above 600 K was much smaller than that on a $Ni/CeO_2(111)$ surface under similar conditions, as seen in Figure 4. Thus, the addition of Ni to CeO_2 largely facilitates the interaction of the surface with methane.

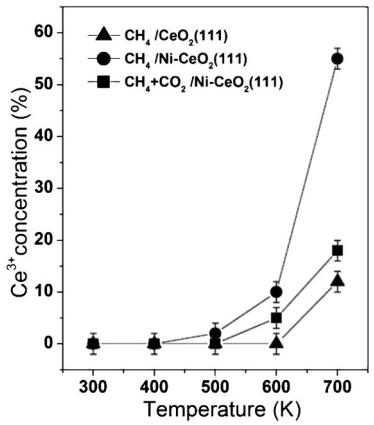

Figure 4. Ce^{3+} concentration measured in XPS as a function of temperature under reaction conditions (i.e. exposure to 100 mTorr of methane or a mixture of 100 mTorr of methane and 100 mTorr of CO_2).

Under a pressure of 100 mTorr of CO_2 at 300 K, the C 1s XPS spectrum for $CeO_2(111)$ or $Ni/CeO_2(111)$ surfaces exhibited a strong feature at 290.2 eV for an adsorbed CO_x species.[14] This feature was seen at 300 K but essentially disappeared when the surfaces were heated to 500 or 700 K. Exposure to CO_2 did not induce any change in the oxidation state of the Ce^{4+} or Ni^{2+} cations. The addition of Ni to $CeO_2(111)$ had a minor effect on the reactivity of the system towards CO_2. On the non-defective $CeO_2(111)$ and $Ni/CeO_2(111)$ surfaces we found no signs for the dissociation of the bonds of CO_2. The reactivity of these surfaces can be increased by the introduction of oxygen vacancies (Vac), $CO_2(g) + Vac \rightarrow CO(a) + O\text{-}Vac$, or H adatoms, $CO_2(g) + H(a) \rightarrow HOCO(a) \rightarrow HO(a) + CO(a)$. Both of them are present on a $Ni/CeO_2(111)$ surface after exposing it to methane.

Figure 5 shows a set of XPS spectra collected for a $Ni/CeO_2(111)$ catalyst under 100 mTorr of CH_4 and 100 mTorr of CO_2 at 300–700 K. At room temperature there was no catalytic activity, but at 700 K the formation of gaseous H_2 and CO was detected in a mass spectrometer. At 300 K, the C 1s region shows peaks for the gaseous reactants, CO_2 and CH_4, and features for adsorbed CO_x and CH_x species. A comparison with the XPS data in Figure 3 for exposure to only CH_4 points to an enhancement in the relative intensity of the signal for CO_x probably as a consequence of the presence of CO_2 in the reactant feed. The signals for CO_x and CH_x

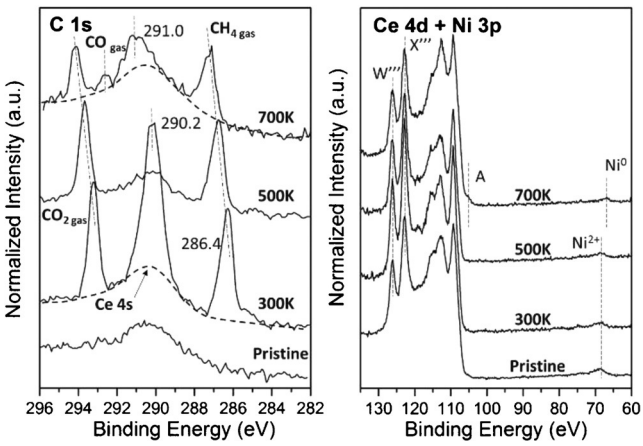

Figure 5. C 1s and Ce 4d + Ni 3p spectra of the $Ni\text{-}CeO_2(111)$ ($\Theta_{Ni} \approx 0.1$ ML) surface under 100 mTorr CH_4 + 100 mTorr of CO_2 at 300, 500, and 700 K.

disappear upon heating from 300 to 500 K. At 500 K, the surface of the catalyst contains Ni^{2+} and Ce^{4+} cations and no catalytic activity was observed. The system became catalytically active at 700 K, when the decomposition products of methane reduced Ni^{2+} to Ni^0 and part of the Ce^{4+} was transformed into Ce^{3+}. Thus, as observed in the in situ XRD data for a powder catalyst (see above), the catalytically active phase contains small particles of metallic nickel on partially reduced ceria. In the C 1s spectrum at 700 K in Figure 5, in addition to the signals for the reactants, there are features for CO gas and a surface CO_x species. The exact identity of this CO_x species is difficult to assign precisely, owing to variations in binding energy as a consequence of changes in work function and band bending with sample reduction, but it could be attributed to CO_2^- or CO_3^- species, which are stable on the surface thanks to the oxygen vacancies generated by the products of methane decomposition. The CO_2 present in gas phase reacts with the surface at 700 K and probably heals a significant fraction of the oxygen vacancies, $CO_2(g) + Vac \rightarrow CO(a) + O\text{-}Vac$. A deconvolution of the Ce 4d spectra in Figure 5 indicates that the net amount of Ce^{3+} formed under a CH_4/CO_2 mixture is much smaller than under pure CH_4 (see a detailed comparison in Figure 4). Under a CH_4/CO_2 mixture, the C generated by the full decomposition of CH_4 does not react with O centers of the oxide, instead, it reacts with the O adatoms produced by the dissociation of CO_2.

An important point to notice in Figure 5 is the lack of signal for adsorbed elemental C or a nickel carbide on the surface. The nickel perturbed by a strong interaction with the ceria is able to dissociate methane but does not generate coke or carbon nanotubes, which is the typical behavior for bulk-like nickel.[8,9,15]

Methane decomposition is frequently cited as the most difficult step for the DRM process.[16] Herein, we apply the spin-polarized DFT + U approach to investigate the dissociative adsorption of methane on Ni deposited on stoichiometric and reduced cerium oxide surfaces, plus the extended Ni(111) surface. The surfaces shown in Figure 2 are quite complex and very difficult to model. They evolve during reaction with part

of the Ni sintering and other part migrating as single atoms into the bulk of ceria.[12,13] To model nickel in close contact with stoichiometric and reduced ceria, we have considered a quarter of a monolayer of Ni atoms deposited on $CeO_2(111)$ and $Ce_2O_3(0001)$ as ideal catalyst surfaces, aiming to elucidate the effects of the two supports in the Ni electronic and chemical properties towards CH_4 adsorption and dissociation as compared to Ni(111). Figures 6a,b a show the Ni/ CeO_2-(111) and Ni/Ce_2O_3(0001) structures, respectively. On CeO_2-(111), the nickel oxidation state is 2+, while on Ce_2O_3(0001) it is 0 (Figure S3). Metallic nickel is partially oxidized on the $CeO_2(111)$ support, which is partially reduced.[17] However, on the reduced $Ce_2O_3(0001)$ support, nickel remains metallic. Hence, these model surfaces mimic the essential features of the experimental catalysts as seen in the XPS data shown in Figure 3 and Figure 5. The molecular binding of methane to Ni(111) is very weak and dissociation, $CH_4(a) \rightarrow CH_3(a) + H(a)$, is difficult due to a large energy barrier.[5,18] Our calculated barrier is approximately 0.9 eV (Figure 6), in agreement with many previous studies.[18] In contrast, supported Ni^{2+} and Ni^0 atoms have an effective CH_4 dissociation barrier that is about 40% and 80% smaller than that for Ni(111), respectively. Therefore, the energy barriers of Ni supported on ceria are much more accessible at room temperature than that on Ni(111), in agreement with the experiments shown in Figure 3 and Figure 5. Furthermore, we notice that chemisorbed CH_4 molecules are 0.35 eV more stable on Ni^0 than Ni^{2+} sites, which increases the probability for reaction on the Ni^0/CeO_{2-x} surfaces.

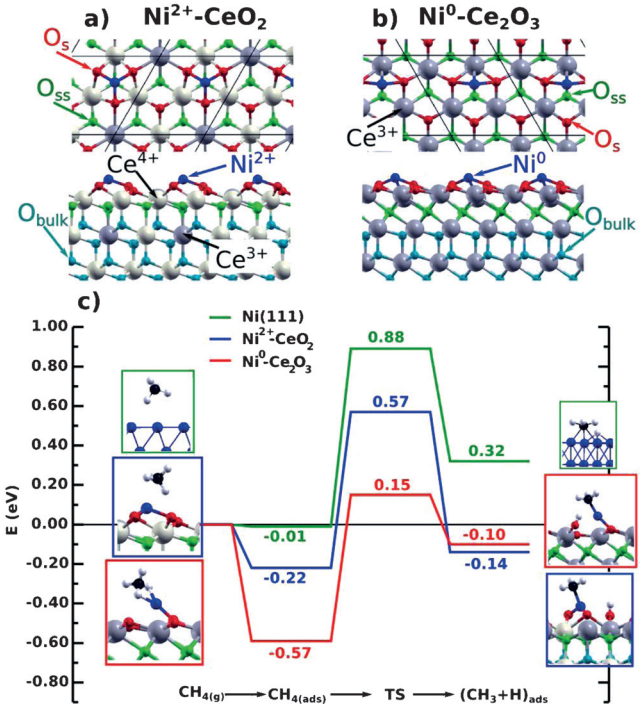

Figure 6. Atomic structure of Ni adsorbed on: a) $CeO_2(111)$ and b) $Ce_2O_3(0001)$. c) Reaction energy profile for the $CH_4 \rightarrow CH_3 + H$ reaction on Ni(111), $Ni^{2+}/CeO_2(111)$, and $Ni^0/Ce_2O_3(0001)$. The structures shown on the left and right of the reaction pathways correspond to the side views of the optimized initial (molecularly adsorbed) and final (dissociated) states used in the search of the transition state (Supporting Information, Figure S4). O_s = surface oxygen atoms, O_{ss} = subsurface oxygen atoms, O_{bulk} = bulk oxygen atoms.

Through strong metal–support interactions, oxides can activate and modify the electronic or chemical properties of a metal.[20,21] Strong metal-support interactions play a key role in the catalytic properties of Ni/CeO_2.[11,12] They enhance the reactivity of Ni towards methane dissociation and probably prevent the deposition of carbon and deactivation during the DRM process. As a result of these interactions, Ni-CeO_2 is a highly efficient, stable and inexpensive catalyst for methane dry reforming at relative low temperatures (700 K).

Acknowledgements

The work carried out at Brookhaven National Laboratory was supported by the US Department of Energy (Chemical Sciences Division, DE-SC0012704). Part of these studies were done at the Advanced Light Source (ALS) which is supported by the US Department of Energy. The theoretical work was supported by the MINECO-Spain (CTQ2012-32928 and CTQ2015-71823-R). P.G.L. thanks CONICET for an external postdoctoral fellowship and G.E. Murgida for helpful discussions. J.C. acknowledges support by the Ramón *y* Cajal Fellowship, the Marie Curie Career Integration Grant FP7-PEOPLE-2011-CIG: Project NanoWGS, and the Royal Society through the Newton Alumnus scheme. The COST action CM1104 is gratefully acknowledged. Computer time provided by the SGAI-CSIC, CESGA, BIFI-ZCAM, IFCA, and the BSC is acknowledged. J.Z. thanks to the support by National Science Foundation (Award Number: CHE1151846) and Wyoming NASA EPSCoR (NASA Grant No. NNX13AB13A).

Keywords: ceria · density functional theory · methane dissociation · nickel · X-ray photoelectron spectroscopy

How to cite: *Angew. Chem. Int. Ed.* **2016**, *55*, 7455–7459
Angew. Chem. **2016**, *128*, 7581–7585

[1] a) D. Pakhare, J. Y. Spivey, *Chem. Soc. Rev.* **2014**, *43*, 7813 – 7837; b) R. Horn, R. Schlogl, *Catal. Lett.* **2015**, *145*, 23 – 39.
[2] Y. H. Hu, E. Ruckenstein, *Adv. Catal.* **2004**, *48*, 297 – 345.
[3] J.-M. Lavoie, *Front. Chem.* **2014**, *2*, 81.
[4] R. H. Crabtree, *Chem. Rev.* **1995**, *95*, 987 – 1007.
[5] T. Choudhary, D. W. Goodman, *J. Mol. Catal. A* **2000**, *163*, 9 – 18.
[6] K. Mette, S. Kühl, H. Düdder, K. Kähler, A. Tarasov, M. Muhler, M. Behrens, *ChemCatChem* **2014**, *6*, 100 – 104.
[7] X. Du, D. Zhang, L. Shi, R. Gao, J. Zhang, *J. Phys. Chem. C* **2012**, *116*, 10009 – 10016.
[8] B. Steinhauer, M. R. Kasireddy, J. Radnik, A. Martin, *Appl. Catal. A* **2009**, *366*, 333 – 341.
[9] S. A. Theofanidis, V. V. Galvita, H. Poelman, G. B. Marin, *ACS Catal.* **2015**, *5*, 3028 – 3039.
[10] Y. Zhou, J. Zhou, *J. Phys. Chem. C* **2012**, *116*, 9544 – 9549.
[11] J. Carrasco, D. López-Duran, Z. Liu, T. Duncho, J. Evans, S. D. Senanayake, E. J. Crumlin, V. Mantolin, J. A. Rodriguez, M. V. Ganduglia-Pirovano, *Angew. Chem. Int. Ed.* **2015**, *54*, 3917 – 3921; *Angew. Chem.* **2015**, *127*, 3989 – 3993.
[12] S. Senanayake, J. Evans, S. Agnoli, L. Barrio, T. Chen, J. Hrbek, J. A. Rodriguez, *Top. Catal.* **2011**, *54*, 34 – 41.
[13] a) A. Caballero, J. P. Holgado, V. M. Gonzalez-de la Cruz, S. E. Habas, T. Herranz, M. Salmeron, *Chem. Commun.* **2010**, *46*, 1097 – 1099; b) D. Kong, J. Zhu, K.-H. Ernst, *J. Phys. Chem. C* **2016**, *120*, 5980 – 5987.
[14] K. Mudiyanselage, S. D. Senanayake, L. Feria, S. Kundu, A. E. Baber, J. Graciani, A. B. Vidal, S. Agnoli, J. Evans, R. Chang, S. Axnanda, Z. Liu, J. F. Sanz, P. Liu, J. A. Rodriguez, D. J. Stacchiola, *Angew. Chem. Int. Ed.* **2013**, *52*, 5101 – 5105; *Angew. Chem.* **2013**, *125*, 5205 – 5209.
[15] K. Otsuka, Y. Abe, N. Kanai, Y. Kobayashi, S. Takenaka, E. Tanabe, *Carbon* **2004**, *42*, 727 – 736.
[16] J. Wei, E. Iglesia, *J. Phys. Chem. B* **2004**, *108*, 4094 – 4103.
[17] J. Carrasco, L. Barrio, P. Liu, J. A. Rodriguez, M. V. Ganduglia-Pirovano, *J. Phys. Chem. C* **2013**, *117*, 8241 – 8250.
[18] a) F. Abild-Pedersen, O. Lytken, J. Engbæk, G. Nielsen, I. Chorkendorff, J. K. Nørskov, *Surf. Sci.* **2005**, *590*, 127 – 137; b) S. Nave, A. K. Tiwari, B. Jackson, *J. Chem. Phys.* **2010**, *132*, 054705; c) B. iang, R. Liu, J. Li, D. Xie, M. Yang, H. Guo, *Chem. Sci.* **2013**, *4*, 3249 – 3254; d) J. Li, E. Croiset, L. Ricardez-Sandoval, *Chem. Phys. Lett.* **2015**, *639*, 205 – 210.
[19] Y. H. Chin, C. Buda, M. Neurock, E. Iglesia, *J. Am. Chem. Soc.* **2013**, *135*, 15425 – 15442.
[20] a) M. Sterrer, T. Risse, U. Martinez Pozzoni, L. Giordano, M. Heyde, H.-P. Rust, G. Pacchioni, H.-J. Freund, *Phys. Rev. Lett.* **2007**, *98*, 096107; b) A. Bruix, J. A. Rodriguez, P. J. Ramirez, S. D. Senanayake, J. Evans, J. B. Park, D. Stacchiola, P. Liu, J. Hrbek, F. Illas, *J. Am. Chem. Soc.* **2012**, *134*, 8968 – 8974; c) A. Bruix, et al., *Angew. Chem. Int. Ed.* **2014**, *53*, 10525 – 10530; *Angew. Chem.* **2014**, *126*, 10693 – 10698; d) V. Simic-Milosevic, M. Heyde, N. Nilius, T. Konig, H.-P. Rust, M. Sterrer, T. Risse, H.-J. Freund, L. Giordano, G. Pacchioni, *J. Am. Chem. Soc.* **2008**, *130*, 7814 – 7815.
[21] a) T. Lunkenbein, J. Schumann, M. Behrens, R. Schlögl, M. G. Willinger, *Angew. Chem. Int. Ed.* **2015**, *54*, 4544 – 4548; *Angew. Chem.* **2015**, *127*, 4627 – 4631; b) J. Schumann, M. Eichelbaum, T. Lunkenbein, N. Thomas, M. C. Álvárez-Galvan, R. Schlögl, M. Behrens, *ACS Catal.* **2015**, *5*, 3260 – 3270.

Received: March 10, 2016
Published online: May 4, 2016

